



Response of electroactive biofilms from real wastewater to metal ion shock in bioelectrochemical systems



Jiexuan Cai^a, Na Yu^a, Fengyi Guan^a, Xixi Cai^a, Rui Hou^b, Yong Yuan^{a,*}

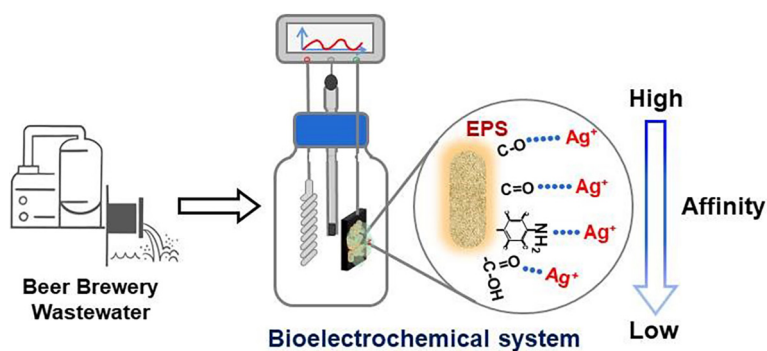
^a Guangzhou Key Laboratory Environmental Catalysis and Pollution Control, Guangdong Key Laboratory of Environmental Catalysis and Health Risk Control, School of Environmental Science and Engineering, Institute of Environmental Health and Pollution Control, Guangdong University of Technology, Guangzhou 510006, China

^b Key Laboratory of Tropical Marine Bio-Resources and Ecology, Guangdong Provincial Key Laboratory of Applied Marine Biology, South China Sea Institute of Oceanology, Chinese Academy of Sciences, Guangzhou 510301, China

HIGHLIGHTS

- EABs from BBW had poorer electrical activity than those from synthetic wastewaters.
- EABs from BBW exhibited higher resistance to Ag⁺ shock than that from glucose.
- Oxygen and nitrogen moieties of proteins and humic acid in EPS played important roles in anti-Ag⁺ shock.

GRAPHICAL ABSTRACT



ARTICLE INFO

Editor: Yifeng Zhang

Keywords:
Real wastewater
Electroactive biofilms
Extracellular polymeric substances
Ag⁺ shock

ABSTRACT

The electrochemical activity of bioelectrochemical systems (BESs) was proven to be dependent on the stability of electroactive biofilms (EABs), but the response of EABs based on real wastewater to external disturbances is not fully known. Herein, we used real wastewater (beer brewery wastewater) as a substrate for culturing EABs and found that current generation, biomass, redox activity and extracellular polymeric substances (EPS) content in those EABs were lower as compared to EABs cultured with synthetic wastewaters (acetate and glucose). However, the EABs from the beer brewery wastewater showed moderate anti-shock resistance capability. The proteins and humic acid in loosely bound EPS (LB-EPS) exhibited a positive linear relationship with current recovery after Ag⁺ shock, indicating the importance of LB-EPS for protecting the EABs. Fluorescence and Fourier transform infrared spectroscopy integrated with two-dimensional correlation spectroscopy verified that the spectra of the protein-like region of LB-EPS changed considerably under the interference of Ag⁺ concentration and the C—O group of humic acid or proteins was mainly responsible for binding with Ag⁺ to attenuate its toxicity to the EABs. This is the first study revealing the underlying molecular mechanism of EABs cultured with real wastewater against external heavy metal shock and provides useful insights into enhancing the application of BESs in future water treatment.

1. Introduction

The bioelectrochemical systems (BESs) are environmentally friendly technology that employ electroactive biofilms (EABs) as catalysts and reac-

tion bodies to achieve simultaneous decontamination and energy production (Logan and Rabaey, 2012). To date, BESs have been explored in a variety of applications ranging from wastewater treatment to energy production, biosensors and bioremediation (Cabrera et al., 2021; Kim et al., 2007; Liu et al., 2004; Nanchariaiah et al., 2015; Srikanth et al., 2018; Zhang et al., 2020a). As the most critical component of BESs, EABs are prone to environmental disturbances, which hinder the bio-

* Corresponding author.
E-mail address: yuanrong@soil.gd.cn (Y. Yuan).

electrocatalytic activity of BESs. Previous studies have shown that the electron transfer pathways and microbial communities of EABs cultured with synthetic wastewater were significantly impacted by external disturbances such as temperature, pH change, hydrodynamic shear, heavy metal shock and antibiotic exposure (Patil et al., 2010; Patil et al., 2011; Wang et al., 2017; Zhang et al., 2020b). In this regard, numerous studies have focused on mitigating the effects of external disturbances to EABs. For example, encapsulating EABs with biocompatible polydopamine to provide protection from extreme acid shock (Du et al., 2017) or modifying EABs with Au-NPs/rGO to enhance the anti-shock ability to phenolic compounds (Li et al., 2021).

Extracellular polymeric substances (EPS) are fundamental parts of EABs as well as the microorganisms that inhabit them, with multiple roles including strengthening bacterial adhesion and promoting the structural development of biofilms (Ras et al., 2011). The abundant components (e.g., proteins, polysaccharides, nucleic acids, and humic substances) with the active groups (e.g., carboxyl, phenol and amino groups) in EPS can provide protective barriers and a nutrient bank for the growth of biofilms (Frederick et al., 2011; Lin et al., 2020; Shou et al., 2018; Xue et al., 2012), which makes the biofilms more resistant to external stresses than individual planktonic cells. EPS can vary in quantity and composition as a result of operational conditions and environmental factors (Li et al., 2008; Zhao et al., 2016), which may affect the ability of biofilms to respond to external disturbances (Gao et al., 2020; Xu and Sheng, 2020). We recently found that EABs produced at 0 V possessed the largest number of EPS and exhibited the highest resistance to Ag^+ stimulation in comparison to those grown under other anode potentials (Hou et al., 2020). Li et al. (2020) found that EABs growing under limited acetate availability decreased the secretion of polysaccharide in EPS, leading to a reduction in the ability to protect the EABs from disintegration by extreme environmental conditions. These studies used synthetic wastewater to provide ideal conditions, but no clear and plausible conclusion has been proposed for the stability of EABs cultured directly on real wastewater. Considering the composition of real wastewater is more complex and diverse than that of synthetic wastewater, it is desirable to investigate the stability of EABs under such conditions as well as to reveal their resistance mechanisms to external shocks.

Herein, the aim of this study was to explore the responses of EABs from real wastewater to Ag^+ shock, using EABs from synthetic wastewater for comparison. EABs were constructed under three different substrates (i.e., beer brewery wastewater, sodium acetate and glucose), where the contents of EPS in the as-formed biofilms were measured. Ag^+ is one of the most toxic metal ions for bacteria and its concentration is expected to substantially increase in the near future due to the growing use of silver nanoparticles (AgNPs) in food, beverages, healthcare and other industries (Zakaria et al., 2018). Beer brewery wastewater was used because it contains organic compounds that are suitable resources for the BESs and has been employed successfully for bioenergy production by BESs (Wang and Ren, 2014). We chose glucose and sodium acetate synthetic wastewaters for comparison because they are typical fermentable and non-fermentable substrates, respectively (Prathiba et al., 2022; Tejedor Sanz et al., 2018). When the biofilms reached maturity, they were treated with Ag^+ solution to investigate the anti-shock characteristics of the EABs. We then established the relationship between EPS components and resistance of EABs, and used fluorescence and Fourier transform infrared (FTIR) combined with two-dimensional correlation spectroscopy (2D-COS) analysis to reveal the binding mechanism of EPS to Ag^+ .

2. Materials and methods

2.1. BES reactors construction and operation

Single-chamber BES reactors were constructed using a 100 mL transparent plexiglass container, where a graphite plate ($1.5 \times 2.0 \times 0.5$ cm) was employed as the working electrode, and titanium wire and a saturated calomel electrode (SCE) were used as the counter electrode and reference

electrode, respectively (Yuvraj and Aranganathan, 2017). The BES reactors were connected to a multichannel potentiostat (CHI 1000C, Chenhua, China), applying a constant potential (0.2 V vs. SCE) at each anode to enrich EABs. The beer brewery wastewater (BBW) used in this experiment was collected from Guangzhou Zhujiang Brewery Co. Ltd. (Guangzhou, China) and stored at 4 °C before use. The sodium acetate (NaAc) synthetic wastewater contained (per L): 1.0 g NaAc, 11.4 g $\text{Na}_2\text{HPO}_4 \cdot 12\text{H}_2\text{O}$, 2.84 g $\text{NaH}_2\text{PO}_4 \cdot 2\text{H}_2\text{O}$, 0.31 g NH_4Cl , 0.13 g KCl, 7.5 mL vitamin solution, and 7.5 mL mineral solution (pH = 6.8). The glucose synthetic wastewater contained (per L): 0.781 g glucose, 11.4 g $\text{Na}_2\text{HPO}_4 \cdot 12\text{H}_2\text{O}$, 2.84 g $\text{NaH}_2\text{PO}_4 \cdot 2\text{H}_2\text{O}$, 0.31 g NH_4Cl , 0.13 g KCl, 7.5 mL vitamin solution, and 7.5 mL mineral solution (pH = 6.8). All BES reactors were inoculated by the effluent of previously well-running BES reactors and run under a constant temperature of 30 °C (Yuan et al., 2011).

2.2. Exposure of EABs to Ag^+ solution

Ag^+ was selected to poison the EABs due to its strong toxicity to bacteria (Ghandour et al., 1988; Silver et al., 2006). The Ag^+ solution (30 mg/L) was obtained by dissolving 0.0472 g AgNO_3 in 1 L deionized water. When EABs grow to maturity (the BESs having generated eight consecutive cycles of current), the anodes were removed and washed using distilled water and then inserted into the Ag^+ solution. After 3 h of exposure, distilled water was used to wash the anodes three times to remove the remaining Ag^+ solution before being re-installed in the BES reactors and fed with fresh nutrient solution. The Ag^+ concentration and exposure time were selected mainly based on previous research (Hou et al., 2020).

2.3. Characterization of EABs

To investigate the electrochemical activity of the anode biofilms, cyclic voltammetry (CV) was performed when the current reached the maximum value (turnover) and the minimum value (non-turnover). The properties of CV were performed by a scan rate of 1 mV/s from -0.8 to $+0.2$ V vs. SCE (Feng et al., 2016). The biomass of biofilms was determined using One Step Bacterial Active Protein Extraction Kit and BCA Protein Assay Kit (Thermo, USA). In order to image the topography and assess the cell viability of the biofilm, the graphite plates attached with biofilm were rinsed in a sterile saline solution to remove the medium, then stained with a LIVE/DEAD BacLight Bacterial Viability Kit (L7012, Thermo Fisher Scientific Inc., USA) in the dark for 20 min, and finally examined by confocal laser scanning microscopy (CLSM) (LSM 800, Carl Zeiss, Germany) (Wang et al., 2016). The three-dimensional (3D) structure of the biofilm was constructed using the ZEN (Blue Edition, Carl Zeiss). The viability (live/total cells) of each biofilm layer was determined based on pixel counts via Comstat 2.1 software (Xue et al., 2012). For each biofilm sample, multiple positions were randomly selected for image acquisition and further image analysis.

2.4. Extraction, quantification and characterization of EPS

To extract EPS from the biofilms, the biofilms were scrapped carefully from the anodes (Cao et al., 2011; Yang et al., 2019a). In brief, the collected biofilms were placed in centrifuge tubes to form 5 mL suspension via 0.9 % NaCl solution. Then an equal volume of preheated solution (70 °C) was added followed by water bath sonication for 2 min and vortex for 2 min and finally centrifugation at 5000g for 15 min. Loosely bound EPS (LB-EPS) was obtained by filtration of the supernatant through 0.22 μm (Cao et al., 2011). The remaining precipitate was re-suspended with 0.9 % NaCl solution, then heated in a 50 °C water bath for 30 min and centrifuged at 5000g for 20 min. The final supernatant filtered through 0.22 μm was collected as tightly bound EPS (TB-EPS) (Yang et al., 2019a). The content of the main components in the collected EPS (proteins, polysaccharides and humic acid) were determined separately. Polysaccharides was measured using the anthrone-sulfuric acid method (Larsson and Törnkvist, 1996), humic acid and proteins were determined through a modified Lowry method (Frolund et al., 1995) and a BCA Protein Assay Kit (Thermo,

USA) (Kang et al., 2014), respectively. The concentrations of polysaccharides, humic acid and proteins were normalized to the biomass of biofilms as mg/g VSS. UV/Vis spectroscopy (UV-2600, Shimadzu, Japan) was used to measure the absorption spectra of the c-type cytochromes in EPS.

2.5. Fluorescence and FTIR measurements

Following the protocol of a previous study (Chen et al., 2015), 2DCOS analysis was performed on synchronous fluorescence and FTIR spectra of LB-EPS with the addition of Ag^+ (0–30 mg/L) as external disturbances. The extracted EPS were first freeze-dried (LGJ-10C, Sihuan, China), then dissolved in ultrapure water and adjusted to a concentration of 15 mg/L (pH 7.0). A series of EPS- Ag^+ gradient concentrations samples were generated by adding appropriate volumes of silver ions and then the test samples were shaken at 25 °C for 12 h to make sure complete equilibration of the reaction and then analyzed using a fluorescence spectrometer (Edinburgh, FLS1000, UK) (Chen et al., 2015; Hur and Lee, 2011). The freeze-dried EPS- Ag^+ samples were homogenized with dried KBr (IR grade), pressed and then measured using an infrared spectrometer (Nicolet iS50R, Thermo-Fisher, USA). Based on the methodology of the Noda and Ozaki report (Noda and Ozaki, 2004), 2DCOS spectra were produced using 2D Shige software (Kwansei-Gakuin University, Japan). More detailed mathematical procedures were described in the SI-1 in Supplementary Materials. Prior to 2DCOS analysis, the FTIR spectra were smoothed and baseline-corrected using OMNIC 8.0 software.

3. Results and discussion

3.1. Electrochemical activity of EABs formed from different substrates

The current response of BESs was recorded by a potentiostat and displayed cyclic current over time once the reactor was reloaded with fresh medium. When the BESs generated stable current for three consecutive cycles, indicating that the BESs have been successfully start-up. As shown in Fig. 1a, the EABs cultured with beer brewery wastewater approached a steady-state current density of $0.5 \pm 0.1 \text{ mA/cm}^2$, which was much lower than that of NaAc ($2.1 \pm 0.1 \text{ mA/cm}^2$) and glucose ($1.1 \pm 0.1 \text{ mA/cm}^2$). Typically, the maximum current density obtained in the BESs using glucose as the substrate was lower than that in BESs fed with acetate due to the loss of electron by means of competing microbes (Lee et al., 2008; Prathiba et al., 2022). Previous studies have also shown that the current generation or coulomb efficiency of the BESs fed with complex real wastewater were generally low due to the fermentable organic matter, non-exoelectrogen invasion, low conductivity, and availability of other electron acceptors (Feng et al., 2011; Yu et al., 2015). Beer brewery wastewater has a high content of organic substances such as carbohydrates that require conversion into smaller molecules to be utilized by electrogenic microorganisms at the anode (Logan et al., 2019). Moreover, the untreated beer brewery wastewater used in this study may contain electron acceptors that compete and disturb the electron accepting function of the anode (Zhao et al., 2020), which might lead to its relatively lower current density. In addition, CV scans under turnover conditions showed similar current

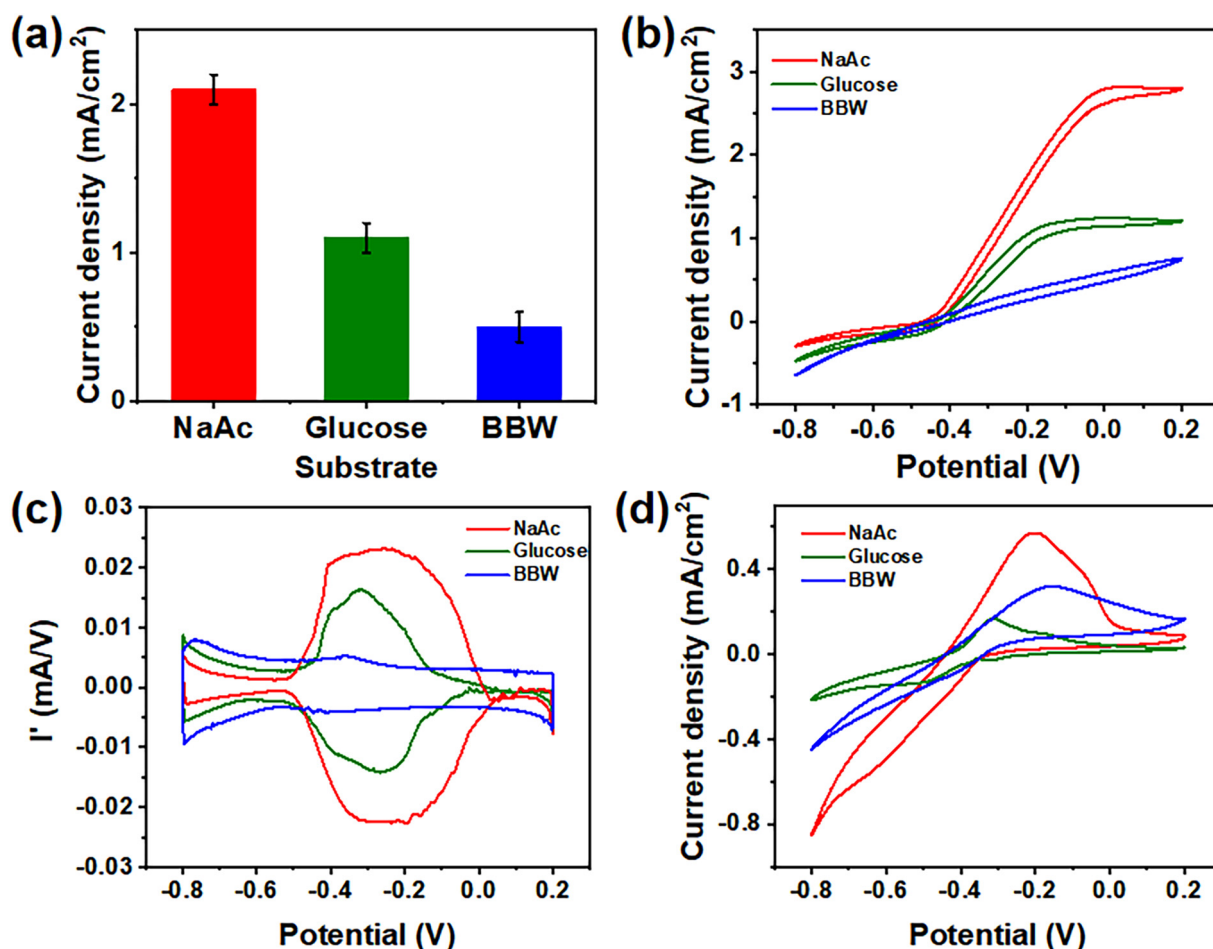


Fig. 1. (a) Maximum current density versus time during formation of the EABs under various substrates; (b) CV scans of EABs under the turnover condition (scan rates: 1 mV/s); (c) the corresponding first derivative analysis of the turnover CV; (d) CV scans of EABs under the non-turnover condition (scan rates: 1 mV/s).

responses (Fig. 1b). The turnover CVs of these EABs were typical sigmoid-shape (Fricke et al., 2008), where showed the ability of substrate oxidation and electron transfer in the sequence of BBW < Glucose < NaAc. The first-order derivative CV (Fig. 1c) showed that the EABs incubated with substrates of sodium acetate and glucose exhibited the increased electrical activities ($I' > 0$) over a similar range of anode potential, while the potential range of the EABs from BBW was significantly different. This indicated that there may be different electron transfer components involved in the real wastewater EABs compared to the EABs from synthetic wastewater (Guo et al., 2021). These results can also be verified by the non-turnover CVs of the EABs (Fig. 1d), where the lowest current response was observed for beer brewery wastewater and the position of the redox pairs was also significantly different from the other EABs. In addition, the biomass of EABs was highly consistent with the variation of current generation (Fig. S1), where the lowest amount of biomass was obtained for the EABs formed from BBW. Overall, as expected, these results suggested that the electrochemical properties of EABs cultured with real BBW were inferior to those of the synthetic wastewater.

3.2. Resistance of various EABs to Ag^+ toxicity

Current recovery ratios of EABs were 74.19 %, 51.04 % and 67.11 % for sodium acetate, glucose and beer brewery wastewater, respectively, after 3 h exposure to Ag^+ solution (Fig. 2). No noticeable drop in current was found when EABs were treated in KNO_3 solution for the same 3 h (Fig. S2), indicating that the decrease in the current was due to Ag^+ exposure rather than caused by the manipulation process (such as moving the electrode) or the toxicity of NO_3^- . Notably, the EABs cultured with beer brewery wastewater had significantly higher anti-shock capability than that with glucose, but was lower than that with acetate.

The change in the EABs viability before and after Ag^+ shock was examined by used of fluorescent staining to distinguish live from dead cells. All EABs were observed to possess a structure of a live outer-layer on top of a dead inner-core layer, which was consistent with previous studies (Hou et al., 2020; Sun et al., 2015). For each substrate, the number of dead cells (red in color) in the EABs became higher after exposure to Ag^+ solution (Fig. 3a), indicating the adverse effect of Ag^+ on bacteria. As shown in Fig. 3b, the viability (live/total cells) of biofilms before and after treatment with Ag^+ showed a comparable trend to the recovery rate of the current (Fig. 2). A viability of 35.8 % was observed for the EABs cultured in BBW, with lower activity than sodium acetate cultured biofilm after Ag^+ shock, but higher than glucose cultured biofilm. Meanwhile, the thinnest EABs was obtained in BBW (Fig. 3c), which was in accordance with its lowest current and biomass. Quantitative analysis of cell viability in each biofilm layer was performed on the Z-stacks captured by CLSM, and all EABs

exhibited more dead cells in the inner layer and more viable cells in the outer layer (Fig. 3c), which may be caused by the proton gradient and mass transfer limitation of electron donors within the biofilm (Yang et al., 2019b). Although the current and biomass obtained from EABs with real BBW as substrate were the lowest, their resistance to Ag^+ shock in regards to electrical activity and cell viability were not the worst.

3.3. EPS production in various EABs and the importance of proteins and humic acid in LB-EPS to protect EABs against Ag^+ toxicity

The EPS, which can be classified as LB-EPS and TB-EPS as far as the state of association with bacterial cells, play a significant role in the protection of biofilms when they are exposed to external stimulation (Fu et al., 2021; Lai et al., 2018; Nocelli et al., 2016). As shown in Fig. 4a, the EPS contents of the EABs from the three substrates differed, where the BBW EABs produced the lowest amounts of LB-EPS and TB-EPS. We further determined the polysaccharides, proteins and humic acid contents in EPS (Fig. 4b and c). The highest content in all three LB-EPS was polysaccharides under the operating parameters of this study, which was different from the previous study with a short operation time (Hou et al., 2020). As the increase in the running time, the thickness of biofilms increased and the resistance to mass transport was enhanced, which stimulated the production of extracellular polysaccharide under this unfavorable condition (Yang et al., 2019b). A previous study have also confirmed that thick membrane-aerated biofilm contained higher content of polysaccharides than proteins (Li et al., 2008).

In addition, the EPS were further evaluated by UV-Vis spectroscopy. All spectra showed a strong absorption band at 409 nm in the oxidized form of EPS and Soret band (419 nm) and Q band (524 and 553 nm) in the reduced form of EPS (Fig. S4), which could be attributed to the characteristics of the oxidized and reduced forms of c-type cytochromes (Heidary et al., 2020; Liu et al., 2011). This suggested that both LB-EPS and TB-EPS fractions of EABs cultured with BBW contained c-type cytochromes, which are the key electron transfer components of electroactive bacteria and are also the main redox substances in the EPS of these organisms (Cao et al., 2011; Tan et al., 2019). As the measured absorbance is proportional to the concentration of c-type cytochromes, the content of c-type cytochromes in the various EPS followed the trend of BBW < Glucose < NaAc, which was consistent with the trends of current generation of the EABs.

Considering that the importance of EPS in protection of biofilms from external stresses (Fu et al., 2021; Lai et al., 2018), we investigated the relationship between EPS components and the current recovery rates from the different EABs. As shown in Fig. 5, each component of TB-EPS and polysaccharides of LB-EPS were poorly correlated with current recovery rate of the biofilms after Ag^+ exposure ($R^2 < 0.55$, $P < 0.05$). However, both the proteins and humic acid of LB-EPS showed significantly positive correlation with the current recovery rate ($R^2 = 0.99$ and 0.99 , respectively; $P < 0.05$). These results demonstrated that the proteins and humic acid of LB-EPS may contribute to more important effects regarding the resistance of EABs. This phenomenon was consistent with the EPS of EABs on various anode potentials under synthetic wastewater condition from our previous study (Hou et al., 2020). In addition, proteins and humic acid in sludge EPS have also been found to show relatively higher ability for metals ions adsorption than polysaccharides (Wei et al., 2019). Compared to TB-EPS, LB-EPS is located closer to the surface of the biofilms. Therefore, as a physical barrier, the proteins and humic acid in LB-EPS may be the dominant compounds in binding with Ag^+ to attenuate its toxicity to EABs.

3.4. The mechanism of EPS of EABs with real BBW binding to Ag^+

To further understand the binding mechanism of LB-EPS cultured with real wastewater to Ag^+ , we used synchronous fluorescence and infrared spectroscopy combined with 2DCOS analysis, which has previously been shown to be a promising approach for elucidating the mechanism of metal-organic interactions (Chen et al., 2015; Yu et al., 2012). Before performing 2DCOS analysis, common one-dimensional synchronous fluorescence and FTIR were employed to initially determine the conformational

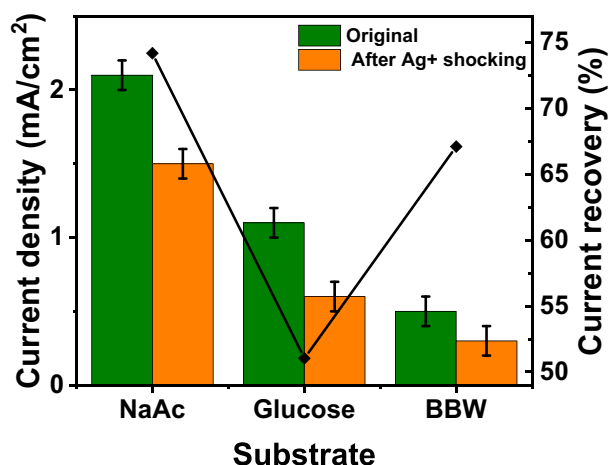


Fig. 2. A comparison of the maximum current density of the EABs before and after Ag^+ exposure (30 mg/L, 3 h) and the corresponding current recovery ratios.

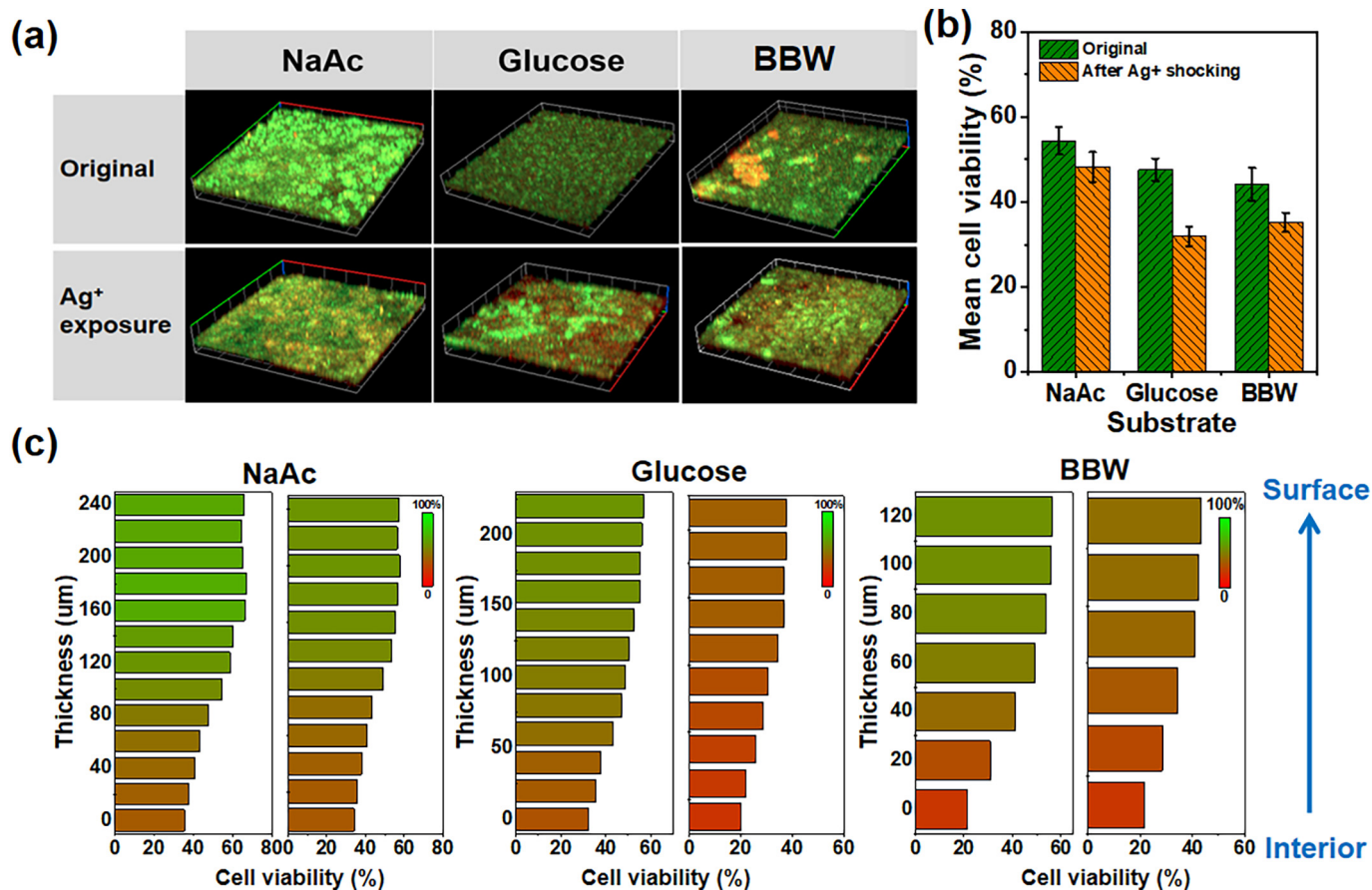


Fig. 3. (a) CLSM of EABs formed under different substrates before and after Ag⁺ exposure (red represents dead cells and green represents live cells); (b) mean cell viability of the EABs before and after Ag⁺ exposure; (c) viability profiles of EABs before (left) and after Ag⁺ exposure (right).

changes caused by EPS binding to Ag⁺. Fig. 6a showed the change in synchronous fluorescence of EPS as different concentrations of Ag⁺ were added. According to previous studies, three fluorescence regions can be roughly assigned to protein-like, fulvic-like, and humic-like corresponding to the wavelength ranges of 250–300, 300–380, and 380–550 nm (Chen et al., 2015; Hur et al., 2011). The EPS of beer brewery wastewater exhibited a higher fluorescence intensity of the protein-like peak than those of the fulvic-like and humic-like peaks (Fig. 6a), suggesting a higher proteins percentage in LB-EPS. With the increase of Ag⁺ concentration, the fluorescence intensity of the protein-like fractions diminished, indicating that the electronic structure changes in the regions were caused by forming complexes with Ag⁺. The main infrared spectral features of LB-EPS appeared over the 1000–2000 cm⁻¹ range, where almost all the information about the vibrations of the constituent skeleton of EPS

can be detected (Abdulla et al., 2010; Yu et al., 2011). Fig. 6b showed that the dominant functional groups of LB-EPS belonged to the C—O—C group of polysaccharides (1085 cm⁻¹), carbonyl C=O group of humic acids or proteins (1390 cm⁻¹) and stretching of C=O in secondary amides (amide I) (1650 cm⁻¹). It is noticeable that these peaks decreased in intensity with the increase of Ag⁺ concentration, meaning that these groups, i.e. carbonyl C=O in humic acids or proteins, C=O stretching in amides and C—O—C in polysaccharides, contributed significantly to the binding of Ag⁺.

To further reliably determine the structural variation of Ag⁺-bound EPS, we used 2DCOS to help improve the spectral resolution by extending the spectrum in a second dimension, allowing us to deconvolve overlapping peaks more easily. According to Fig. 6c, the synchronous 2DCOS maps displayed one predominant autopeak (275/275 nm) along the diagonal

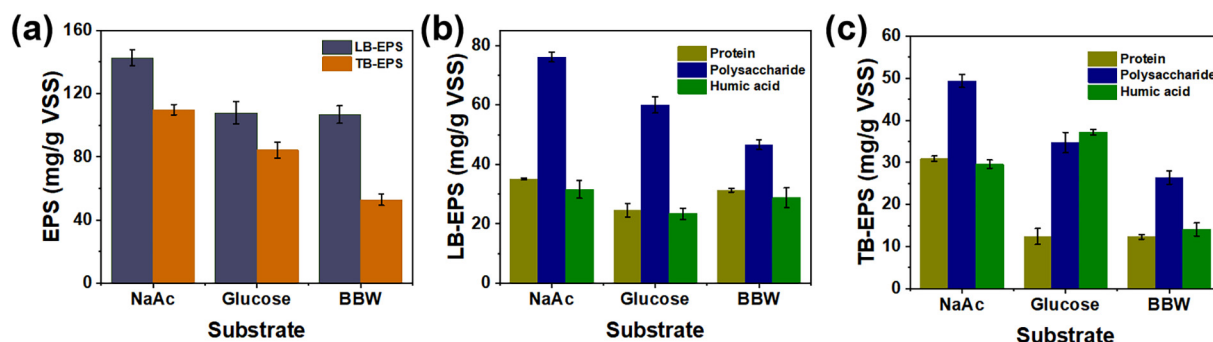


Fig. 4. (a) LB-EPS and TB-EPS contents of the EABs formed under various substrates; EPS of electroactive biofilms under different substrates for LB-EPS (b) and TB-EPS fractions (c), respectively.

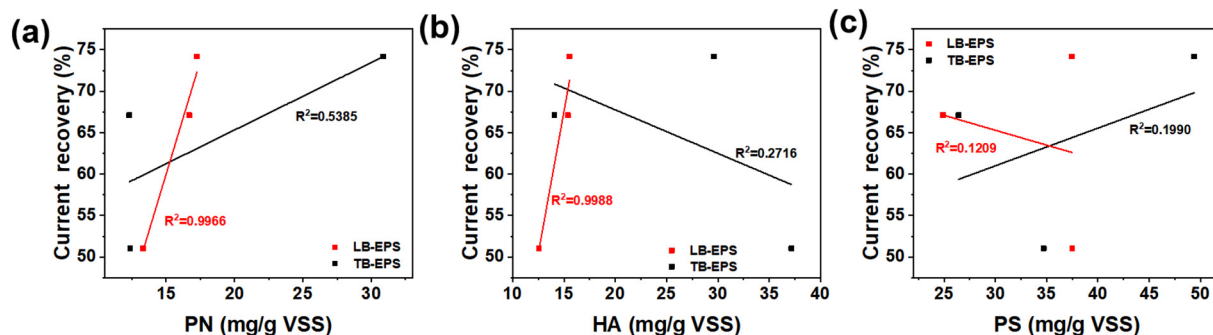


Fig. 5. Plots showing the correlation between the current recovery and content of LB-EPS and TB-EPS fractions: (a) proteins (PN); (b) humic acid (HA); (c) polysaccharides (PS).

line and a small cross-peak centered at 330 nm, suggesting that significant changes in the spectra within the protein-like region occurred under the interference of the Ag^+ concentration change. The cross-peak was positive, indicating that the spectra had the same decreasing trend. Moreover, the cross-peaks centered at 275 nm and 330 nm in the asynchronous map were positive. According to Noda's rule (Noda and Ozaki, 2004), the change followed the order of 275 nm > 330 nm. That is, Ag^+ binds with EPS components in the following order: protein-like region > fulvic-like region. For 2DCOS-FTIR, the synchronous 2DCOS map showed two autopeaks centered at 1087 cm^{-1} and 1390 cm^{-1} , with cross-peaks centered at 1600 cm^{-1} , 1640 cm^{-1} , and 1765 cm^{-1} (Fig. 6e). The symbols of these cross-peaks are given in Table S1. The peak at 1390 cm^{-1} changed the most, followed by the peak at 1087 cm^{-1} , with all cross-peaks being positive. This result confirmed that C—O of humic acid or protein and C—O—C of polysaccharides were potential moieties for the binding reaction with Ag^+ in LB-EPS. The asynchronous 2DCOS-FTIR map displayed five positive and five negative cross-peaks (Fig. 6f and Table S1). According to Noda's rule (Noda and Ozaki, 2004), the order of functional groups

bound with Ag^+ can be derived: $1390\text{ cm}^{-1} > 1765\text{ cm}^{-1} > 1600\text{ cm}^{-1} > 1087\text{ cm}^{-1} > 1640\text{ cm}^{-1}$, that is, C—O of humic acid or proteins > C=O of polysaccharides > N—H of amide > C—O—C of polysaccharides > C=O of amides.

Similar analysis was also performed in LB-EPS cultured with glucose synthetic wastewater with different Ag^+ concentrations as interference (Fig. S6 and Table S2). LB-EPS of glucose showed fewer binding sites compared to that of sodium acetate and beer brewery wastewater (SI-2 in Supplementary Materials), which may be the reason for the lower resistance. Previous studies have shown that *Geobacter* species are frequently found to be abundant in acetate-fed BESs (Dhar et al., 2016a; Dhar et al., 2016b; Torres et al., 2009), whereas a syntrophic cooperation between fermentative microorganisms and electroactive bacteria is predominant when fed with glucose (Li et al., 2016). Zakaria et al. (2018) found that electroactive bacteria (e.g., *Geobacter* spp.) have a higher tolerance to AgNPs toxicity compared to fermentative bacteria. In this regard, the anode biofilm in acetate fed MEC could maintain its electrochemical performance after exposure to AgNPs. However, when a fermentable substrate (i.e., glucose) was

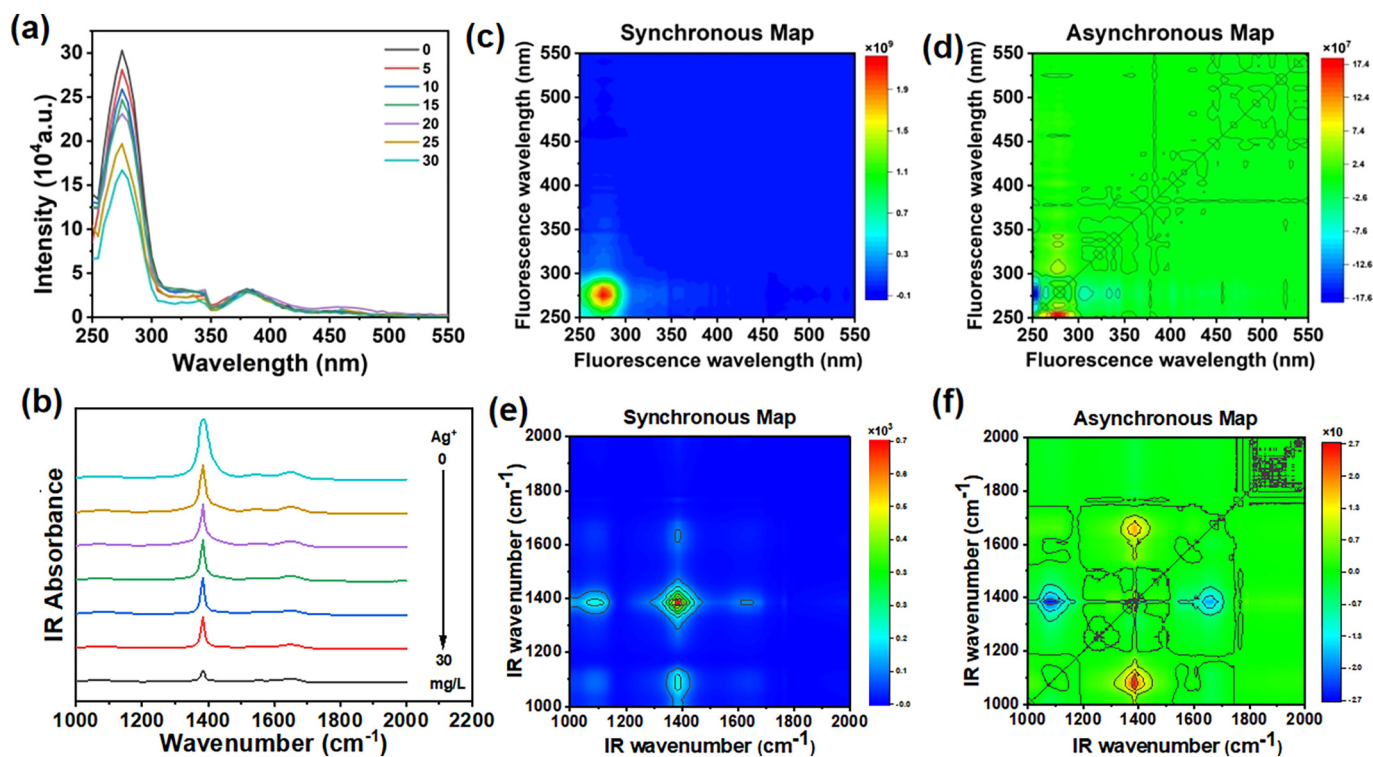


Fig. 6. LB-EPS cultured with beer brewery wastewater with (a) changes in the fluorescence spectra with addition of Ag^+ concentrations (0, 5, 10, 15, 20, 25 and 30 mg/L); (b) changes in the FTIR with increasing Ag^+ concentrations from 0 to 30 mg/L; synchronous (c) and asynchronous (d) 2D-COS generated from the fluorescence spectra; synchronous (e) and asynchronous (f) 2D-COS generated from the FTIR.

used as a substrate, the lower tolerance of fermentative bacteria to the toxicity of AgNPs resulted in the disruption of the synthetic partnership between electrobacteria and fermentative bacteria in the biofilm, which affected the overall performance of the MEC (Zakaria and Dhar, 2020). The release of Ag⁺ has been defined as the main antibacterial mechanism of AgNPs (Levard et al., 2012; Yin et al., 2011). Therefore, it is reasonable to suppose that this is also the reason for the stronger resistance to Ag⁺ shock in sodium acetate-fed EABs than in glucose-fed EABs in our BESs. Considering that EPS were identified as the main defense mechanism against heavy metal ions toxicity, our results are consistent with this statement not only in the current recovery rate, but also in the number of EPS binding sites. However, the complexity of the real wastewater inevitably leads to a more diverse biofilm community in addition to electroactive and fermenting bacteria. This diversity is not positive for electroactivity, but it is perhaps the community diversity that eventually showed a positive effect on resistance to toxic shock. In this study, fermentation-based synthetic wastewater did not show better resistance to Ag⁺ impact, but real beer brewery wastewater contained fermentable and non-fermentable substrates showed more resistance than expected.

4. Conclusions

This study found that the EABs cultured from real beer brewery wastewater had the lowest current generation, biomass, redox activity, and EPS content compared to EABs cultured with synthetic wastewaters, but the resistance to Ag⁺ impact was not the worst. Correlation analysis showed that the proteins and humic acids of LB-EPS may contribute the most to the resistance of EABs to Ag⁺ toxicity. Spectroscopy integrated with 2DCOS analysis elucidated that LB-EPS of the EABs from real beer brewery wastewater followed a sequence of C—O of humic acid or proteins > C=O of polysaccharides > N—H of amide > C—O—C of polysaccharides > C=O of amides for binding to Ag⁺. These findings extend the understanding of interactions between metal ions and electroactive biofilms, particularly fed with a real wastewater substrate. The present study reveals for the first time the underlying mechanisms of EABs cultured with real wastewater for resistance to external metal ions shock. However, the experiment only used beer wastewater as well as Ag⁺ as model substrate and model heavy metal. More types of real wastewater and metal ions are needed in future to provide comprehensive understanding on the anti-shock characteristics of EABs from real wastewaters.

CRedit authorship contribution statement

Jiexuan Cai: Conceptualization, Methodology, Writing – original draft. **Na Yu:** Formal analysis, Software, Investigation. **Fengyi Guan:** Methodology, Software. **Xixi Cai:** Writing – review & editing. **Rui Hou:** Writing – review & editing. **Yong Yuan:** Writing – review & editing, Project administration, Supervision.

Declaration of competing interest

The authors declare no competing interests.

Acknowledgments

This work was supported by National Natural Science Foundation of China (21876032, 41877045, and 42177270) and the fellowship of China Postdoctoral Science Foundation (No. 2021M690728).

Appendix A. Supplementary data

Supplementary data to this article can be found online at <https://doi.org/10.1016/j.scitotenv.2022.157158>.

References

- Abdulla, H.A.N., Minor, E.C., Hatcher, P.G., 2010. Using two-dimensional correlations of 13C NMR and FTIR to investigate changes in the chemical composition of dissolved organic matter along an estuarine transect. *Environ. Sci. Technol.* 44, 8044–8049. <https://doi.org/10.1021/es100898x>.
- Cabrera, J., Irfan, M., Dai, Y., Zhang, P., Zong, Y., Liu, X., 2021. Bioelectrochemical system as an innovative technology for treatment of produced water from oil and gas industry: a review. *Chemosphere* 285, 131428. <https://doi.org/10.1016/j.chemosphere.2021.131428>.
- Cao, B., Shi, L., Brown, R.N., Xiong, Y., Fredrickson, J.K., Romine, M.F., et al., 2011. Extracellular polymeric substances from *Shewanella* sp HRCR-1 biofilms: characterization by infrared spectroscopy and proteomics. *Environ. Microbiol.* 13, 1018–1031. <https://doi.org/10.1111/j.1462-2920.2010.02407.x>.
- Chen, W., Habibul, N., Liu, X.Y., Sheng, G.P., Yu, H.Q., 2015. FTIR and synchronous fluorescence heterospectral two-dimensional correlation analyses on the binding characteristics of copper onto dissolved organic matter. *Environ. Sci. Technol.* 49, 2052–2058. <https://doi.org/10.1021/es5049495>.
- Dhar, B.R., Ryu, H., Ren, H., Domingo, J.W.S., Chae, J., Lee, H.S., 2016a. High biofilm conductivity maintained despite anode potential changes in a *Geobacter*-enriched biofilm. *ChemSusChem* 9, 3485–3491. <https://doi.org/10.1002/cssc.201601007>.
- Dhar, B.R., Ryu, H., Santo Domingo, J.W., Lee, H.S., 2016b. Ohmic resistance affects microbial community and electrochemical kinetics in a multi-anode microbial electrochemical cell. *J. Power Sources* 331, 315–321. <https://doi.org/10.1016/j.jpowsour.2016.09.055>.
- Du, Q., Li, T., Li, N., Wang, X., 2017. Protection of electroactive biofilm from extreme acid shock by polydopamine encapsulation. *Environ. Sci. Technol. Lett.* 4, 345–349. <https://doi.org/10.1021/acs.estlett.7b00242>.
- Feng, C., Liu, Y., Li, Q., Che, Y., Li, N., Wang, X., 2016. Quaternary ammonium compound in anolyte without functionalization accelerates the startup of bioelectrochemical systems using real wastewater. *Electrochim. Acta* 188, 801–808. <https://doi.org/10.1016/j.electacta.2015.12.069>.
- Feng, Y., Yang, Q., Wang, X., Liu, Y., Lee, H., Ren, N., 2011. Treatment of biodiesel production wastes with simultaneous electricity generation using a single-chamber microbial fuel cell. *Bioresour. Technol.* 102, 411–415. <https://doi.org/10.1016/j.biortech.2010.05.059>.
- Frederick, M.R., Kuttler, C., Hense, B.A., Eberl, H.J., 2011. A mathematical model of quorum sensing regulated EPS production in biofilm communities. *Theor. Biol. Med. Model.* 8, 8. <https://doi.org/10.1186/1742-4682-8-8>.
- Fricke, K., Harnisch, F., Schroeder, U., 2008. On the use of cyclic voltammetry for the study of anodic electron transfer in microbial fuel cells. *Energy Environ. Sci.* 1, 144–147. <https://doi.org/10.1039/b802363h>.
- Frolund, B., Griebe, T., Nielsen, P.H., 1995. Enzymatic activity in the activated-sludge floc matrix. *Appl. Microbiol. Biotechnol.* 43, 755–761. <https://doi.org/10.1007/BF00164784>.
- Fu, Q.L., Zhong, C.J., Qing, T., Du, Z.Y., Li, C.C., Fei, J.J., et al., 2021. Effects of extracellular polymeric substances on silver nanoparticle bioaccumulation and toxicity to *Triticum aestivum* L. *Chemosphere* 280, 130863. <https://doi.org/10.1016/j.chemosphere.2021.130863>.
- Gao, X., Deng, R., Lin, D., 2020. Insights into the regulation mechanisms of algal extracellular polymeric substances secretion upon the exposures to anatase and rutile TiO₂ nanoparticles. *Environ. Pollut.* 263, 114608. <https://doi.org/10.1016/j.envpol.2020.114608>.
- Ghandour, W., Hubbard, J.A., Deistung, J., Hughes, M.N., Poole, R.K., 1988. The uptake of silver ions by *Escherichia coli* K12: toxic effects and interaction with copper ions. *Appl. Microbiol. Biotechnol.* 28, 559–565. <https://doi.org/10.1007/BF00250412>.
- Guo, J.H., Yang, G.Q., Zhuang, Z., Mai, Q.J., Li, Z., 2021. Redox potential-induced regulation of extracellular polymeric substances in an electroactive mixed community biofilm. *Sci. Total Environ.* 797. <https://doi.org/10.1016/j.scitotenv.2021.149207>.
- Heidary, N., Kornienko, N., Kalathil, S., Fang, X., Ly, K.H., Greer, H.F., et al., 2020. Disparity of cytochrome utilization in anodic and cathodic extracellular electron transfer pathways of *Geobacter sulfurreducens* biofilms. *J. Am. Chem. Soc.* 142, 5194–5203. <https://doi.org/10.1021/jacs.9b13077>.
- Hou, R., Luo, C., Zhou, S., Wang, Y., Yuan, Y., Zhou, S., 2020. Anode potential-dependent protection of electroactive biofilms against metal ion shock via regulating extracellular polymeric substances. *Water Res.* 178, 115845. <https://doi.org/10.1016/j.watres.2020.115845>.
- Hur, J., Jung, K.Y., Jung, Y.M., 2011. Characterization of spectral responses of humic substances upon UV irradiation using two-dimensional correlation spectroscopy. *Water Res.* 45, 2965–2974. <https://doi.org/10.1016/j.watres.2011.03.013>.
- Hur, J., Lee, B.M., 2011. Characterization of binding site heterogeneity for copper within dissolved organic matter fractions using two-dimensional correlation fluorescence spectroscopy. *Chemosphere* 83, 1603–1611. <https://doi.org/10.1016/j.chemosphere.2011.01.004>.
- Kang, F., Alvarez, P.J., Zhu, D., 2014. Microbial extracellular polymeric substances reduce Ag⁺ to silver nanoparticles and antagonize bactericidal activity. *Environ. Sci. Technol.* 48, 316–322. <https://doi.org/10.1021/es403796x>.
- Kim, M., Hyun, M.S., Gadd, G.M., Kim, H.J., 2007. A novel biomonitoring system using microbial fuel cells. *J. Environ. Monit.* 9, 1323–1328. <https://doi.org/10.1039/b713114c>.
- Lai, C.Y., Dong, Q.Y., Chen, J.X., Zhu, Q.S., Yang, X., Chen, W.D., et al., 2018. Role of extracellular polymeric substances in a methane based membrane biofilm reactor reducing vanadate. *Environ. Sci. Technol.* 52, 10680–10688. <https://doi.org/10.1021/acs.est.8b02374>.
- Larsson, G., Törnkvist, M., 1996. Rapid sampling, cell inactivation and evaluation of low extracellular glucose concentrations during fed-batch cultivation. *J. Biotechnol.* 49, 69–82. [https://doi.org/10.1016/0168-1656\(96\)01534-9](https://doi.org/10.1016/0168-1656(96)01534-9).
- Lee, H.S., Parameswaran, P., Kato Marcus, A., Torres, C.I., Rittmann, B.E., 2008. Evaluation of energy-conversion efficiencies in microbial fuel cells (MFCs) utilizing fermentable and non-fermentable substrates. *Water Res.* 42, 1501–1510. <https://doi.org/10.1016/j.watres.2007.10.036>.
- Levard, C., Hotze, E.M., Lowry, G.V., Brown, G.E., 2012. Environmental transformations of silver nanoparticles: impact on stability and toxicity. *Environ. Sci. Technol.* 46, 6900–6914. <https://doi.org/10.1021/es2037405>.

- Li, B., Sun, J.D., Tang, C., Zhou, J., Wu, X.Y., Jia, H.H., et al., 2021. Coordinated response of Au-NPs/rGO modified electroactive biofilms under phenolic compounds shock: comprehensive analysis from architecture, composition, and activity. *Water Res.* 189, 116589. <https://doi.org/10.1016/j.watres.2020.116589>.
- Li, T., Bai, R., Liu, J., 2008. Distribution and composition of extracellular polymeric substances in membrane-aerated biofilm. *J. Biotechnol.* 135, 52–57. <https://doi.org/10.1016/j.biortech.2008.02.011>.
- Li, T., Zhou, Q., Zhou, L., Yan, Y., Liao, C., Wan, L., et al., 2020. Acetate limitation selects Geobacter from mixed inoculum and reduces polysaccharide in electroactive biofilm. *Water Res.* 177, 115776. <https://doi.org/10.1016/j.watres.2020.115776>.
- Li, Y., Zhang, Y., Liu, Y., Zhao, Z., Zhao, Z., Liu, S., et al., 2016. Enhancement of anaerobic methanogenesis at a short hydraulic retention time via bioelectrochemical enrichment of hydrogenotrophic methanogens. *Bioresour. Technol.* 218, 505–511. <https://doi.org/10.1016/j.biortech.2016.06.112>.
- Lin, H., Wang, C., Zhao, H., Chen, G., Chen, X., 2020. A subcellular level study of copper speciation reveals the synergistic mechanism of microbial cells and EPS involved in copper binding in bacterial biofilms. *Environ. Pollut.* 263, 114485. <https://doi.org/10.1016/j.envpol.2020.114485>.
- Liu, H., Ramnarayanan, R., Logan, B.E., 2004. Production of electricity during wastewater treatment using a single chamber microbial fuel cell. *Environ. Sci. Technol.* 38, 2281–2285. <https://doi.org/10.1021/es034923g>.
- Liu, Y., Kim, H., Franklin, R.R., Bond, D.R., 2011. Linking spectral and electrochemical analysis to monitor c-type cytochrome redox status in living Geobacter sulfurreducens biofilms. *ChemPhysChem* 12, 2235–2241. <https://doi.org/10.1002/cphc.201100246>.
- Logan, B.E., Rabaey, K., 2012. Conversion of wastes into bioelectricity and chemicals by using microbial electrochemical technologies. *Science* 337, 686–690. <https://doi.org/10.1126/science.1217412>.
- Logan, B.E., Rossi, R., Ragab, A.a., Saikaly, P.E., 2019. Electroactive microorganisms in bioelectrochemical systems. *Nat. Rev. Microbiol.* 17, 307–319. <https://doi.org/10.1038/s41579-019-0173-x>.
- Nancharaiya, Y.V., Venkata Mohan, S., Lens, P.N.L., 2015. Metals removal and recovery in bioelectrochemical systems: a review. *Bioresour. Technol.* 195, 102–114. <https://doi.org/10.1016/j.biortech.2015.06.058>.
- Nocelli, N., Bogino, P.C., Banchio, E., Giordano, W., 2016. Roles of extracellular polysaccharides and biofilm formation in heavy metal resistance of rhizobia. *Materials* 9. <https://doi.org/10.3390/ma9060418>.
- Noda, I., Ozaki, Y., 2004. *Two-dimensional Correlation Spectroscopy: Applications in Vibrational and Optical Spectroscopy*.
- Patil, S.A., Harnisch, F., Kapadnis, B., Schröder, U., 2010. Electroactive mixed culture biofilms in microbial bioelectrochemical systems: the role of temperature for biofilm formation and performance. *Biosens. Bioelectron.* 26, 803–808. <https://doi.org/10.1016/j.bios.2010.06.019>.
- Patil, S.A., Harnisch, F., Koch, C., Hübschmann, T., Fetzer, I., Carmona Martínez, A.A., et al., 2011. Electroactive mixed culture derived biofilms in microbial bioelectrochemical systems: the role of pH on biofilm formation, performance and composition. *Bioresour. Technol.* 102, 9683–9690. <https://doi.org/10.1016/j.biortech.2011.07.087>.
- Prathiba, S., Kumar, P.S., Vo, D.V.N., 2022. Recent advancements in microbial fuel cells: a review on its electron transfer mechanisms, microbial community, types of substrates and design for bio-electrochemical treatment. *Chemosphere* 286, 131856. <https://doi.org/10.1016/j.chemosphere.2021.131856>.
- Ras, M., Lefebvre, D., Derlon, N., Paul, E., Girbal-Neuhauser, E., 2011. Extracellular polymeric substances diversity of biofilms grown under contrasted environmental conditions. *Water Res.* 45, 1529–1538. <https://doi.org/10.1016/j.watres.2010.11.021>.
- Shou, W., Kang, F., Lu, J., 2018. Nature and value of freely dissolved EPS ecosystem services: insight into molecular coupling mechanisms for regulating metal toxicity. *Environ. Sci. Technol.* 52, 457–466. <https://doi.org/10.1021/acs.est.7b04834>.
- Silver, S., Phung, L.T., Silver, G., 2006. Silver as biocides in burn and wound dressings and bacterial resistance to silver compounds. *J. Ind. Microbiol. Biotechnol.* 33, 627–634. <https://doi.org/10.1007/s10295-006-0139-7>.
- Srikanth, S., Kumar, M., Puri, S.K., 2018. Bio-electrochemical system (BES) as an innovative approach for sustainable waste management in petroleum industry. *Bioresour. Technol.* 265, 506–518. <https://doi.org/10.1016/j.biortech.2018.02.059>.
- Sun, D., Cheng, S., Wang, A., Li, F., Logan, B.E., Cen, K., 2015. Temporal-spatial changes in viabilities and electrochemical properties of anode biofilms. *Environ. Sci. Technol.* 49, 5227–5235. <https://doi.org/10.1021/acs.est.5b00175>.
- Tan, B., Zhou, S., Wang, Y., Zhang, B., Zhou, L., Yuan, Y., 2019. Molecular insight into electron transfer properties of extracellular polymeric substances of electroactive bacteria by surface-enhanced Raman spectroscopy. *Sci. China Technol. Sci.* 62, 1679–1687. <https://doi.org/10.1007/s11431-018-9437-0>.
- Tejedor Sanz, S., Fernandez Labrador, P., Hart, S., Torres, C.I., Esteve Nunez, A., 2018. Geobacter dominates the inner layers of a stratified biofilm on a fluidized anode during brewery wastewater treatment. *Front. Microbiol.* 9. <https://doi.org/10.3389/fmicb.2018.00378>.
- Torres, C.I., Kraljalmik Brown, R., Parameswaran, P., Marcus, A.K., Wanger, G., Gorby, Y.A., et al., 2009. Selecting anode-respiring bacteria based on anode potential: phylogenetic, electrochemical, and microscopic characterization. *Environ. Sci. Technol.* 43, 9519–9524. <https://doi.org/10.1021/es902165y>.
- Wang, H., Ren, Z.J., 2014. Bioelectrochemical metal recovery from wastewater: a review. *Water Res.* 66, 219–232. <https://doi.org/10.1016/j.watres.2014.08.013>.
- Wang, X., Zhou, L., Lu, L., Lobo, F.L., Li, N., Wang, H., et al., 2016. Alternating current influences anaerobic electroactive biofilm activity. *Environ. Sci. Technol.* 50, 9169–9176. <https://doi.org/10.1021/acs.est.6b00813>.
- Wang, Y.R., Gong, L., Jiang, J.K., Chen, Z.G., Yu, H.Q., Mu, Y., 2017. Response of anodic biofilm to hydrodynamic shear in two-chamber bioelectrochemical systems. *Electrochim. Acta* 258, 1304–1310. <https://doi.org/10.1016/j.electacta.2017.11.187>.
- Wei, L., Li, J., Xue, M., Wang, S., Li, Q., Qin, K., et al., 2019. Adsorption behaviors of Cu²⁺, Zn²⁺ and Cd²⁺ onto proteins, humic acid, and polysaccharides extracted from sludge EPS: sorption properties and mechanisms. *Bioresour. Technol.* 291, 121868. <https://doi.org/10.1016/j.biortech.2019.121868>.
- Xu, J., Sheng, G.P., 2020. Microbial extracellular polymeric substances (EPS) acted as a potential reservoir in responding to high concentrations of sulfonamides shocks during biological wastewater treatment. *Bioresour. Technol.* 313, 123654. <https://doi.org/10.1016/j.biortech.2020.123654>.
- Xue, Z., Sendamangalam, V.R., Gruden, C.L., Seo, Y., 2012. Multiple roles of extracellular polymeric substances on resistance of biofilm and detached clusters. *Environ. Sci. Technol.* 46, 13212–13219. <https://doi.org/10.1021/es3031165>.
- Yang, G., Lin, J., Zeng, E.Y., Zhuang, L., 2019a. Extraction and characterization of stratified extracellular polymeric substances in geobacter biofilms. *Bioresour. Technol.* 276, 119–126. <https://doi.org/10.1016/j.biortech.2018.12.100>.
- Yang, G.Q., Huang, L.Y., Yu, Z., Liu, X.M., Chen, S.S., Zeng, J.X., et al., 2019b. Anode potentials regulate Geobacter biofilms: new insights from the composition and spatial structure of extracellular polymeric substances. *Water Res.* 159, 294–301. <https://doi.org/10.1016/j.watres.2019.05.027>.
- Yin, L., Cheng, Y., Espinasse, B., Colman, B.P., Auffan, M., Wiesner, M., et al., 2011. More than the ions: the effects of silver nanoparticles on *lolium multiflorum*. *Environ. Sci. Technol.* 45, 2360–2367. <https://doi.org/10.1021/es103995x>.
- Yu, G.H., Tang, Z., Xu, Y.C., Shen, Q.R., 2011. Multiple fluorescence labeling and two dimensional FTIR–13C nmr heterospectral correlation spectroscopy to characterize extracellular polymeric substances in biofilms produced during composting. *Environ. Sci. Technol.* 45, 9224–9231. <https://doi.org/10.1021/es201483f>.
- Yu, G.H., Wu, M.J., Wei, G.R., Luo, Y.H., Ran, W., Wang, B.R., et al., 2012. Binding of organic ligands with Al(III) in dissolved organic matter from soil: implications for soil organic carbon storage. *Environ. Sci. Technol.* 46, 6102–6109. <https://doi.org/10.1021/es3002212>.
- Yu, J., Park, Y., Kim, B., Lee, T., 2015. Power densities and microbial communities of brewery wastewater-fed microbial fuel cells according to the initial substrates. *Bioprocess Biosyst. Eng.* 38, 85–92. <https://doi.org/10.1007/s00449-014-1246-x>.
- Yuan, Y., Zhao, B., Zhou, S., Zhong, S., Zhuang, L., 2011. Electrocatalytic activity of anodic biofilm responses to pH changes in microbial fuel cells. *Bioresour. Technol.* 102, 6887–6891. <https://doi.org/10.1016/j.biortech.2011.04.008>.
- Yuvraj, C., Aranganathan, V., 2017. MFC-an approach in enhancing electricity generation using electroactive biofilm of dissimilatory iron-reducing (DIR) bacteria. *Arab. J. Sci. Eng.* 42, 2341–2347. <https://doi.org/10.1007/s13369-017-2529-8>.
- Zakaria, B.S., Barua, S., Sharaf, A., Liu, Y., Dhar, B.R., 2018. Impact of antimicrobial silver nanoparticles on anode respiring bacteria in a microbial electrolysis cell. *Chemosphere* 213, 259–267. <https://doi.org/10.1016/j.chemosphere.2018.09.060>.
- Zakaria, B.S., Dhar, B.R., 2020. Changes in syntrophic microbial communities, EPS matrix, and gene-expression patterns in biofilm anode in response to silver nanoparticles exposure. *Sci. Total Environ.* 734, 139395. <https://doi.org/10.1016/j.scitotenv.2020.139395>.
- Zhang, S., Yang, Y.L., Lu, J., Zuo, X.J., Yang, X.L., Song, H.L., 2020a. A review of bioelectrochemical systems for antibiotic removal: efficient antibiotic removal and dissemination of antibiotic resistance genes. *J. Water Process. Eng.* 37. <https://doi.org/10.1016/j.jwpe.2020.101421>.
- Zhang, Z., Qu, Y., Li, S., Feng, K., Cai, W., Yin, H., et al., 2020b. Florfenicol restructured the microbial interaction network for wastewater treatment by microbial electrolysis cells. *Environ. Res.* 183, 109145. <https://doi.org/10.1016/j.envres.2020.109145>.
- Zhao, F., Heidrich, E.S., Curtis, T.P., Dolfling, J., 2020. Understanding the complexity of wastewater: the combined impacts of carbohydrates and sulphate on the performance of bioelectrochemical systems. *Water Res.* 176, 115737. <https://doi.org/10.1016/j.watres.2020.115737>.
- Zhao, L., She, Z., Jin, C., Yang, S., Guo, L., Zhao, Y., et al., 2016. Characteristics of extracellular polymeric substances from sludge and biofilm in a simultaneous nitrification and denitrification system under high salinity stress. *Bioprocess Biosyst. Eng.* 39, 1375–1389. <https://doi.org/10.1007/s00449-016-1613-x>.